Available online at www.sciencedirect.com
ScienceDirect
Optics Communications 266 (2006) 159–163
OPTICS COMMUNICATIONS
www.elsevier.com/locate/optcom

Engineering absolute band gap in anisotropic hexagonal photonic crystals

B. Rezaei *, M. Kalafi

Research Institute for Applied Physics and Astronomy, Tabriz University, Tabriz 51665-163, Iran

Received 18 January 2006; received in revised form 18 April 2006; accepted 26 April 2006

Abstract

We analyze the band gap spectra of two-dimensional anisotropic photonic crystals created by a hexagonal lattice of rods covered by an interfacial layer (e.g. tellurium tubes). Using the plane-wave numerical expansion method, we study the modification of the band gap spectrum when the rods are infiltrated with other material, and discuss the optimization strategies leading to the maximum value of the absolute band gap.

PACS: 42.70.Qs; 78.20.Ci; 78.20.Bh

Keywords: Photonic crystal; Photonic band gap; Anisotropic tellurium

1. Introduction

Photonic band gap materials (also known as photonic crystals) are expected to revolutionize the fields of integrated optics and micro-photonics due to an efficient control of the electromagnetic radiation they provide, in such a way as semiconductors control the behaviors of the electron [1,2]. One of the key properties of photonic crystals is their ability to trap light for certain frequency ranges due to the existence of absolute photonic band gaps in the propagation spectra. Engineering the value of the absolute band gaps is crucial for a design of useful optical devices based on the light trapping and reflection in such structures.

Most of the studies of the absolute band gaps in two-dimensional photonic crystals have been restricted by engineering the lattice geometry (e.g. triangular, square, or hexagonal) or by a change of the shape, cross-section, and orientation of the elementary units of the structure, i.e. rods or holes. To the best of our knowledge, only a few recent studies addressed the important issue how an additional interfacial (or cladding) layer affects the values and properties of photonic gaps [3–5]. In particular, it was noticed that such interfacial layers can appear around holes in macro-porous silicon after etching, and they can have a dramatic effect of the properties of the band gap spectra of photonic crystals [4]. In addition, the use of tellurium hollow rods [5] may have a dramatic effect of the absolute band gap due to the properties of the photonic crystals made of anisotropic dielectrics [6].

More recently, the interest in the study of the properties of complex photonic crystals with interfacial layers has been enhanced by the effort to model the void-based photonic crystals created by a femtosecond laser-driven micro-explosion method where a change in the refractive index in the region surrounding the void dots that form the bcc structures is verified experimentally [7]. In addition, the recently suggested class of the so-called annular photonic crystals [8], where dielectric rods are embedded into air holes of larger radius, fit the same category of complex structures where the air space can be regarded as an additional, interfacial layer.

The aim of this paper is twofold. First, we extend the previously published results by studying an important case

* Corresponding author.
E-mail address: b.rezaei@tabrizu.ac.ir (B. Rezaei).

0030-4018/$ - see front matter © 2006 Elsevier B.V. All rights reserved.
doi:10.1016/j.optcom.2006.04.035

of hexagonal two-dimensional photonic crystals created by a lattice of hollow dielectric rods, also assuming that the hollow rods are filled by another material. Second, we consider the hollow rods made of tellurium and study how the anisotropy of the dielectric material can affect the band gap properties and the value of the absolute band gap.

2. Lattice and model description

To determine absolute PBGs in periodic dielectric structures, we study the propagation of light from Maxwell's equations. In inhomogeneous dielectric materials the Maxwell's equation for the magnetic field yields [9,10]:

$$\nabla \times \left[\frac{1}{\varepsilon(\vec{r})}\nabla \times H(\vec{r})\right] = \frac{\omega^2}{c^2}H(\vec{r}) \tag{1}$$

where ω is the frequency of light and c is the light velocity. The dielectric constant $\varepsilon(\vec{r})$ is a periodic function of $\vec{r}$ in x–y plane and satisfies the condition $\varepsilon(\vec{r}+\vec{R}) = \varepsilon(\vec{r})$, $\vec{R}$ denotes real space lattice vectors. Since $\varepsilon(\vec{r})$ is periodic, we can use Bloch's theorem to expand the $H(\vec{r})$ as a sum of plane waves [9,11]:

$$H(\vec{r}) = \sum_{\vec{G}}\sum_{\lambda=1}^{2} h_{\vec{G},\lambda}\hat{e}_\lambda e^{i(\vec{k}+\vec{G})\cdot\vec{r}} \tag{2}$$

where $\vec{k}$ is a wave vector in the first Brillouin zone and $\vec{G}$ is a 2D reciprocal lattice vector, $\hat{e}_\lambda$ $(\lambda = 1, 2)$ are orthogonal unit vectors perpendicular to $\vec{k}+\vec{G}$. So, Eq. (1) is expressed as a linear matrix equation for the dispersion of EM waves [12]:

$$\sum_{\vec{G}'} H_{\vec{G},\vec{G}'}\begin{pmatrix} h_{\vec{G}',1} \\ h_{\vec{G}',2}\end{pmatrix} = \frac{\omega^2}{c^2}\begin{pmatrix} h_{\vec{G},1} \\ h_{\vec{G},2}\end{pmatrix} \tag{3}$$

where

$$H_{\vec{G},\vec{G}'} = |\vec{k}+\vec{G}||\vec{k}+\vec{G}'|\eta(\vec{G}-\vec{G}')\begin{bmatrix} \hat{e}_2\cdot\hat{e}'_2 & -\hat{e}_2\cdot\hat{e}'_1 \\ -\hat{e}_1\cdot\hat{e}'_2 & \hat{e}_1\cdot\hat{e}'_1\end{bmatrix} \tag{4}$$

$\eta(\vec{G})$ is the Fourier transform of the inverse of $\varepsilon(\vec{r})$, and plays a key role in determination of photonic band structure. We study a periodic array of dielectric rods that their extension direction is parallel to the z-axis and the intersection of these rods with the x–y plane form a 2D periodic dielectric structure. In this case, the Fourier coefficients are given by

$$\eta(\vec{G}) = \frac{1}{\Omega}\int_{\text{cell}} \varepsilon^{-1}(\vec{r})e^{-i\vec{G}\cdot\vec{r}}\,d\vec{r} \tag{5}$$

Here we designate the surface of unit cell by Ω. In a 2D photonic crystal $\vec{k}+\vec{G}$ is in the x–y plane for all $\vec{G}$, so we can choose all $\hat{e}_1$ and $\hat{e}_2$ vectors parallel to the z direction and in the x–y plane, respectively. In this case $\hat{e}_2\cdot\hat{e}'_1 = \hat{e}_1\cdot\hat{e}'_2 = 0$. For light incident perpendicular to the rod axis, the matrix Eq. (4) decouple into two scalar problems, corresponding to two polarizations. In the case of E-polarization ($E(\vec{r})$ is parallel to the rod axis), $h_{\vec{G},1} = 0$ for all $\vec{G}$ and we have

$$\sum_{\vec{G}'} |\vec{k}+\vec{G}||\vec{k}+\vec{G}'|\eta(\vec{G}-\vec{G}')h_{\vec{G}',2} = \frac{\omega^2}{c^2}h_{\vec{G},2} \tag{6}$$

For the H-polarization ($H(\vec{r})$ is in the rod axis), $h_{\vec{G},2} = 0$ for all $\vec{G}$ and the eigenvalue equation becomes

$$\sum_{\vec{G}'} (\vec{k}+\vec{G})\cdot(\vec{k}+\vec{G}')\eta(\vec{G}-\vec{G}')h_{\vec{G}',1} = \frac{\omega^2}{c^2}h_{\vec{G},1} \tag{7}$$

The structure under consideration and the corresponding first Brillouin zone is shown in Fig. 1. We have considered a hexagonal structure of circular shape rods with dielectric constant ε_r of inner rod and anisotropic outer shell, embedded periodically in a background of dielectric constant ε_b. The anisotropic outer shell layer has two different principle-refractive indices as ordinary-refractive index n_o and extraordinary-refractive index n_e.

We assume that the extraordinary axis is parallel to the z-axis. In this configuration, the eigenequations for the E- and H-polarization modes are the same as those for

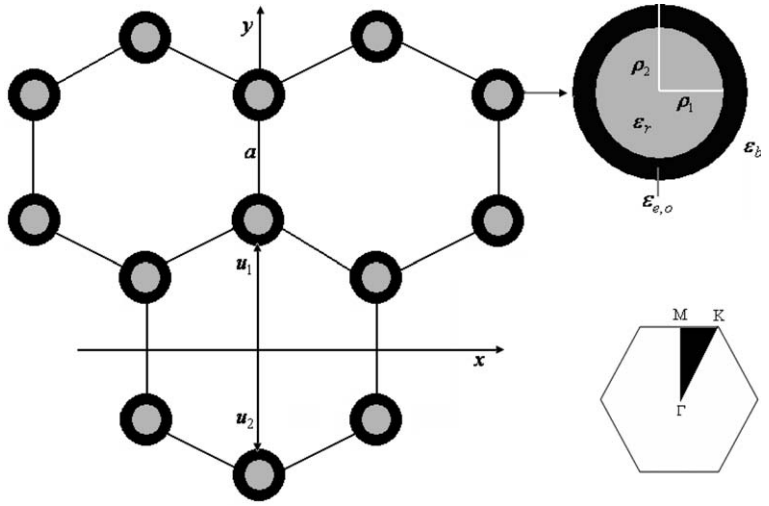

Fig. 1. Model of a 2D hexagonal structure of circular anisotropic Te rods consist of an inner rod with dielectric constant ε_r embedded in a uniform background ε_b and the first Brillouin zone.

the isotropic photonic crystals, except that the dielectric indices of anisotropic outer shell are n_e and n_o for E- and H-polarizations, respectively. The Corresponding dielectric constant is expressed as

$$\frac{1}{\varepsilon(\vec{r})} = \frac{1}{\varepsilon_b} + \left(\frac{1}{\varepsilon_r} - \frac{1}{\varepsilon_b}\right) \sum_i \sum_{\vec{R}} P_{rod}(\vec{r} - u_i - \vec{R}) + \left(\frac{1}{\varepsilon_{e,o}} - \frac{1}{\varepsilon_b}\right) \sum_i \sum_{\vec{R}} P_{shell}(\vec{r} - u_i - \vec{R}) \quad (8)$$

where $\varepsilon_e = n_e^2$ and $\varepsilon_o = n_o^2$, P_{rod} and P_{shell} describe the probability of finding the inner rod and shell, respectively, and can be expressed as

$$P_{rod}(\vec{r}) = \begin{cases} 1, & \vec{r} \in R_{rod} \\ 0, & \vec{r} \notin R_{rod} \end{cases} \quad P_{shell}(\vec{r}) = \begin{cases} 1, & \vec{r} \in R_{shell} \\ 0, & \vec{r} \notin R_{shell} \end{cases} \quad (9)$$

where R_{rod} and R_{shell} are the regions in the x–y plane defined by the cross-section of the inner rod and outer shell, respectively. The unit cell of hexagonal lattice contain two rods located at positions u_1 and u_2, where $u = u_1 = -u_2 = a(0,1)$, and a is lattice constant. The Fourier transform of $\varepsilon^{-1}(\vec{r})$ for structures with a unit cell including some identical cylinders located at u_i positions, is given by

$$\eta(\vec{G}) = \frac{1}{\varepsilon_b}\delta_{\vec{G},0} + S(\vec{G})\eta_c(\vec{G}) \quad (10)$$

where $S(\vec{G})$ is the structure factor

$$S(\vec{G}) = \sum_j e^{-i\vec{G}\cdot u_j} \quad (11)$$

and $\eta_c(\vec{G})$ correspond to the Fourier transform for a cylinder centered at the origin. For the hexagonal structure of shelled circular rods, the Fourier coefficients can be written as

$$\eta(\vec{G}) = \begin{cases} \frac{1}{\varepsilon_b} + \frac{2\pi\rho_1^2}{\Omega}\left(\frac{1}{\varepsilon_r} - \frac{1}{\varepsilon_b}\right) + \frac{2\pi}{\Omega}(\rho_2^2 - \rho_1^2)\left(\frac{1}{\varepsilon_{e,o}} - \frac{1}{\varepsilon_b}\right), & \vec{G} = 0 \\ \frac{4\pi}{\Omega G}\cos(\vec{G}\cdot u)\left\{\left(\frac{1}{\varepsilon_r} - \frac{1}{\varepsilon_b}\right)\rho_1 J_1(\rho_1 G) + \left(\frac{1}{\varepsilon_{e,o}} - \frac{1}{\varepsilon_b}\right)[\rho_2 J_1(\rho_2 G) - \rho_1 J_1(\rho_1 G)]\right\}, & \vec{G} \neq 0 \end{cases} \quad (12)$$

where $J_1(x)$ is the Bessel function of the first kind. ρ_1 and ρ_2 are the radius of the inner rod and the outer radius of the shell layer, respectively.

3. Results and discussion

For this study a 2D hexagonal photonic crystal of circular rods consisting of an inner rod with dielectric constant ε_r and anisotropic outer shell aligned in a uniform background with dielectric constant ε_b has been considered.

The band structure of 2D photonic crystal is obtained numerically by solving Eqs. (6) and (7). A total of 441 plane waves were used in these calculations, which ensures sufficient convergence for the frequencies of interest. Our main goal here is to study the modification of the band gap spectrum and the value of the absolute band gap when the thickness of outer shell layer varies, as well as when the rods are infiltrated with other materials.

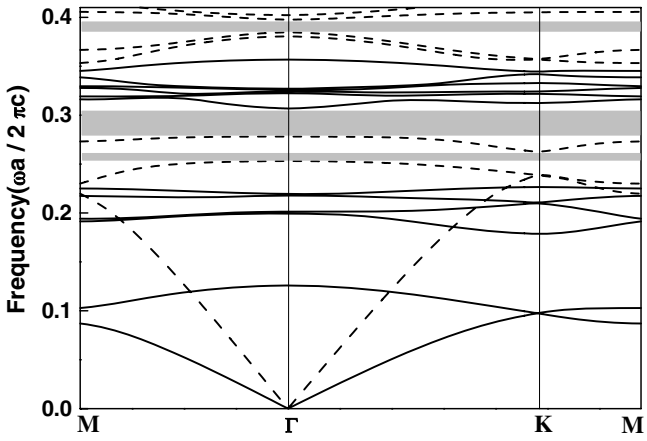

Fig. 2. Photonic band structure for hexagonal lattice of solid Te rods in air background at optimum value of $\rho_2 = 0.33a$ for E-polarization (solid) and H-polarization (dashed) modes.

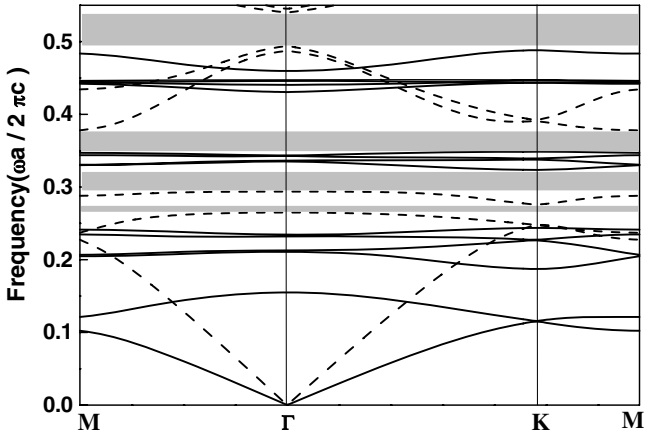

Fig. 3. Photonic band structure for hexagonal lattice of Te rods in air background at optimum values of $\rho_1 = 0.13a$ and $\rho_2 = 0.33a$ for E-polarization (solid) and H-polarization (dashed) modes.

Table 1
Maximum absolute PBG width $\Delta\omega$ and the corresponding lower and upper frequencies (ω_1, ω_2) for Optimum inner rod radius ρ_1 at different core dielectric constant ε_r

ε_r	ρ_{1-opt}/a	$\Delta\omega(2\pi c/a)$	$\omega_1(2\pi c/a)$	$\omega_2(2\pi c/a)$
1	0.13	0.0458	0.4942	0.54
5	0.23	0.0531	0.3888	0.4418
10	0.23	0.0643	0.3384	0.4027
15	0.23	0.0688	0.3094	0.3782
18	0.24	0.0698	0.299	0.3689
20	0.24	0.072	0.2901	0.3621
25	0.26	0.0777	0.2698	0.3475
27	0.265	0.0798	0.2622	0.3420
28	0.265	0.0795	0.26	0.3395
30	0.265	0.076	0.2586	0.3346
35	0.3	0.063	0.2552	0.3182
40	0.33	0.0503	0.2516	0.3019
43	0.33	0.0436	0.2496	0.2931

We have chosen Te as the anisotropic outer shell, which has a positive uniaxial crystal with principle indices of $n_e = 6.2$ and $n_o = 4.8$. The dielectric constant of background is $\varepsilon_b = 1$. In this structure two geometrical parameters ρ_1 and ρ_2 are treated as adjustable parameters to obtain the maximum absolute PBG.

First we consider the case when $\rho_1 = 0$ (solid Te rods), i.e., there is no core dielectric constant. Fig. 2 shows the photonic band structure for optimum value of $\rho_2 = 0.33a$. This frequency spectrum displays several absolute PBGs, and a relatively large one at lower frequency with maximum normalized width of $\Delta\omega = 0.0287(2\pi c/a)$ which lies between 0.278 and $0.3068(2\pi c/a)$ frequencies.

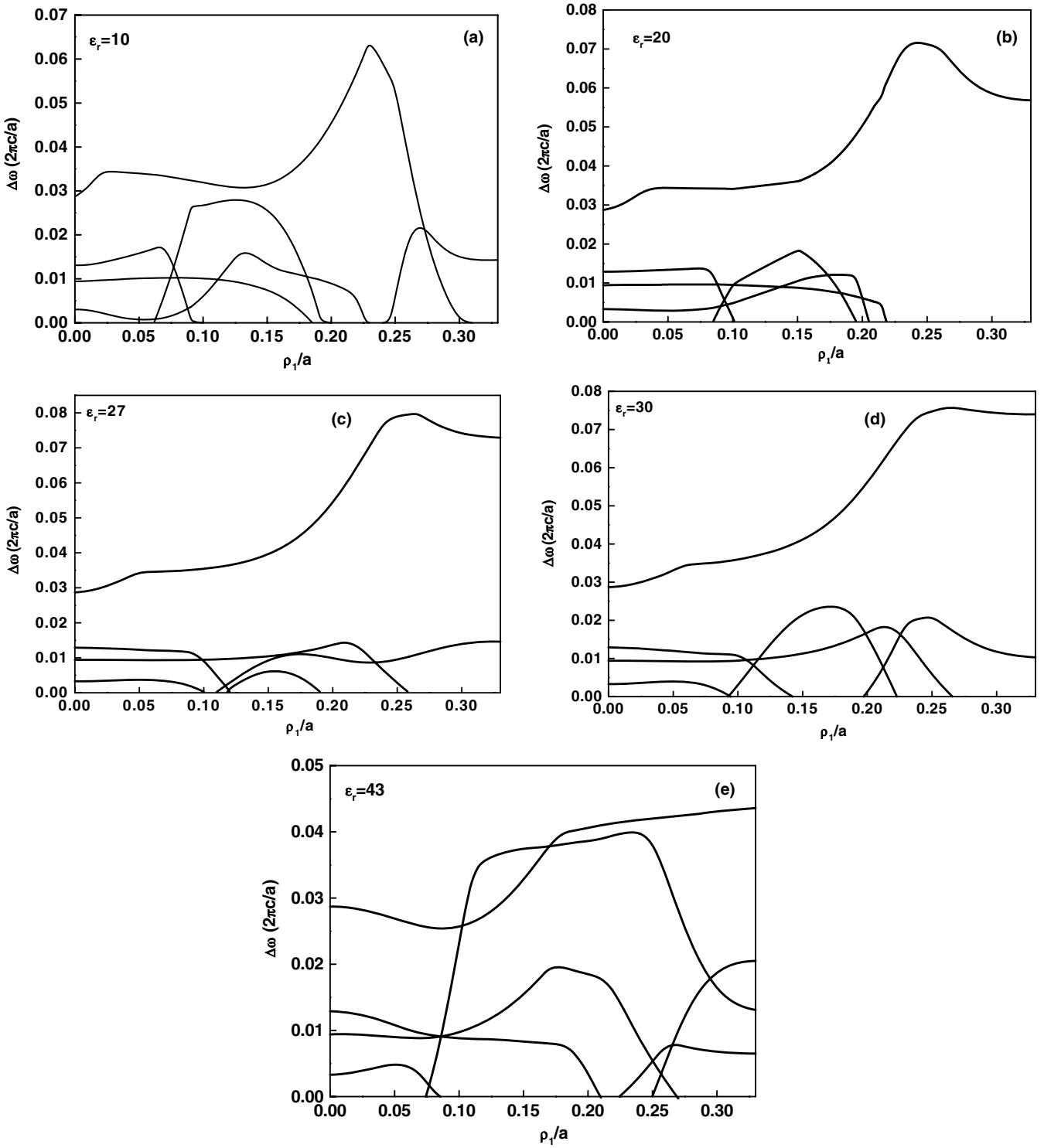

Fig. 4. Width of absolute photonic band gaps versus inner rod radius ρ_1 for hexagonal lattice of Te rods consist of different core dielectric constants: (a) $\varepsilon_r = 10$, (b) $\varepsilon_r = 20$, (c) $\varepsilon_r = 27$, (d) $\varepsilon_r = 30$ and (e) $\varepsilon_r = 43$ at fixed value of $\rho_2 = 0.33a$.

At next step, the inner space of rods is filled with other materials. In this case, for a given value of ε_r, the inner rod radius ρ_1 is optimized to obtain the maximum absolute PBG at optimum value of $\rho_2 = 0.33a$. As an example, the frequency spectrum in the case of hollow Te rods, $\varepsilon_r = 1$, with optimum inner rod radius of $\rho_1 = 0.13a$ is shown in Fig. 3. The largest absolute PBG reaches its maximum normalized width of $\Delta\omega = 0.0458(2\pi c/a)$ and lies between 0.4942 and $0.54(2\pi c/a)$ frequencies. So, compared with the case of solid Te rods, the maximum absolute PBG has been increased and shifted to higher normalized frequencies.

Finally, we study how the filling of inner space of the Te rods with different dielectric constants may change the size and position of the maximum absolute PBG. This achieved by optimizing the inner rod radius ρ_1 for different values of ε_r as listed in Table 1.

Table 1 shows the calculated normalized maximum absolute PBG width, $\Delta\omega$, and its corresponding lower and upper frequencies (ω_1 and ω_2) at fixed optimum value of $\rho_2 = 0.33a$ for several values of ε_r with related optimum inner rod radius $\rho_{1-\mathrm{opt}}$. It can be seen that by increasing the magnitude of core dielectric constant, ε_r, the maximum absolute PBG occurs at low frequency region and the optimum inner rod radius, $\rho_{1-\mathrm{opt}}$, increases slowly. Also, it can be seen that for $\varepsilon_r > 35$ the optimum value of inner rod radius reaches the optimum value of outer rod radius ($\rho_1 = \rho_2$), i.e. the outer shell completely disappears. Fig. 4 summarizes the results for some values of the core dielectric constants of $\varepsilon_r = 10$, 20, 27, 30, and 43. This figure shows the normalized width of the all absolute PBGs as a function of the inner rod radius ρ_1 at optimum outer radius of $\rho_2 = 0.33a$ for a given inner dielectric constant ε_r. It can be seen that as the value of ε_r increases, the position of the maximum absolute PBG shifts towards higher values of ρ_1 and occurs at low frequency regions. Also, it can be seen that by increasing the value of ε_r, the width of maximum absolute PBG increases and reaches its maximum at $\varepsilon_r = 27$, as shown in Fig. 4(c). For $\varepsilon_r > 27$ the width of maximum absolute PBG decreases and occurs at higher values of ρ_1, where for $\varepsilon_r > 35$ it occurs at $\rho_1 = \rho_2$ and the outer shell completely disappears (Fig. 4(d) and (e)). The main result is that the greatest absolute PBG with normalized width of $\Delta\omega = 0.0798(2\pi c/a)$ is achieved for $\varepsilon_r = 27$ at optimum inner rod radius of $\rho_1 = 0.265a$ which lies between 0.2622 and $0.3420(2\pi c/a)$ frequencies.

Also, for the purposes of comparison, in Fig. 5 the normalized width of the maximum absolute PBG is plotted versus the inner rod radius, ρ_1, for several values of ε_r.

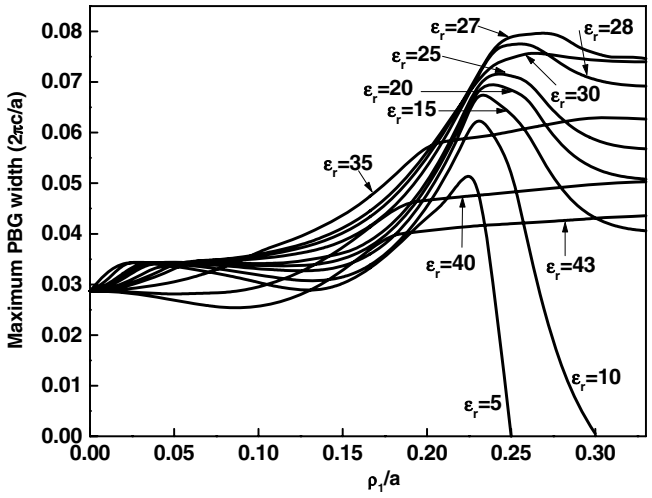

Fig. 5. Width of maximum absolute PBG as a function of inner rod radius ρ_1 for different core dielectric constants at optimum value of $\rho_2 = 0.33a$.

4. Conclusion

In conclusion, we have analyzed band gap spectra of two-dimensional anisotropic photonic crystals created by a hexagonal lattice of rods covered by an interfacial layer (e.g. thin tellurium tubes). Using the plane-wave numerical expansion method, we have studied different aspects of the modification of the band gap spectrum when the thickness of covering layer varies, as well as when the tubes are infiltrated with other material. We have discussed and demonstrated several optimization strategies leading to the maximum value of the absolute band gap in such anisotropic photonic crystals.

Acknowledgements

The authors are indebted to Yuri Kivshar (Canberra, Australia) for useful discussions and suggestions.

References

[1] E. Yablonovitch, Phys. Rev. Lett. 58 (1987) 2059.
[2] S. John, Phys. Rev. Lett. 58 (1987) 2486.
[3] T. Pan, Z.-Y. Li, Solid State Commun. 128 (2003) 187.
[4] T. Trifonov, L.F. Marsal, A. Rodriguez, J. Pallares, R. Alcubilla, Phys. Rev. B 70 (2004) 195108.
[5] T. Pan, F. Zhuang, Z.-Y. Li, Solid State Commun. 129 (2004) 501.
[6] Z.Y. Li, B.Y. Gu, G.Z. Yang, Phys. Rev. Lett. 81 (1998) 2574.
[7] G. Zhou, M.J. Ventura, M. Gu, A.F. Mattews, Yu.S. Kivshar, Opt. Express 13 (2005) 4390.
[8] Hamza Kurt, D.S. Citrin, Opt. Express 13 (2005) 10316.
[9] J.D. Joannopoulos, R.D. Meade, J.N. Winn, Photonic Crystals: Molding the Flow of Light, Princeton University Press, Princeton, 1995.
[10] M. Plihal, A.A. Maradudin, Phys. Rev. B 44 (1991) 8565.
[11] K.M. Ho, C.T. Chan, C.M. Soukoulis, Phys. Rev. Lett. 65 (1990) 3152.
[12] K. Busch, S. John, Phys. Rev. E 58 (1998) 3896.